

One-dimensional massless Dirac bands in semiconductor superlattices

Carosella, F.; Wacker, Andreas; Ferreira, R.; Bastard, G.

Published in:

Physical Review B (Condensed Matter and Materials Physics)

DOI:

10.1103/PhysRevB.89.235301

2014

Document Version: Publisher's PDF, also known as Version of record

Link to publication

Citation for published version (APA):

Carosella, F., Wacker, A., Ferreira, R., & Bastard, G. (2014). One-dimensional massless Dirac bands in semiconductor superlattices. *Physical Review B (Condensed Matter and Materials Physics)*, *89*(23), Article 235301. https://doi.org/10.1103/PhysRevB.89.235301

Total number of authors:

General rights

Unless other specific re-use rights are stated the following general rights apply:

Copyright and moral rights for the publications made accessible in the public portal are retained by the authors and/or other copyright owners and it is a condition of accessing publications that users recognise and abide by the legal requirements associated with these rights.

- Users may download and print one copy of any publication from the public portal for the purpose of private study or research.

 • You may not further distribute the material or use it for any profit-making activity or commercial gain
- You may freely distribute the URL identifying the publication in the public portal

Read more about Creative commons licenses: https://creativecommons.org/licenses/

Take down policy

If you believe that this document breaches copyright please contact us providing details, and we will remove access to the work immediately and investigate your claim.

One-dimensional massless Dirac bands in semiconductor superlattices

F. Carosella,^{1,*} A. Wacker,² R. Ferreira,¹ and G. Bastard¹

¹Laboratoire Pierre Aigrain, ENS-CNRS UMR 8551, Universités P. et M. Curie and Paris-Diderot, 24, rue Lhomond, 75231 Paris Cedex 05, France

²Mathematical Physics, Lund University, Box 118, S-22100 Lund, Sweden (Received 31 October 2013; published 3 June 2014)

Semiconductor superlattices may display dispersions that are degenerate either at the zone center or zone boundary [G. Bastard, *Wave Mechanics Applied to Semiconductor Heterostructures*, Monographies de Physique (Les Éditions de Physique, Les Ulis, 1988); C. Sirtori, F. Capasso, D. L. Sivco, and A. Y. Cho, Appl. Phys. Lett. **64**, 2982 (1994)]. We show that they are linear upon the wave vector in the vicinity of the crossing point. This establishes a realisation of massless Dirac bands within semiconductor materials. We show that the eigenstates and the corresponding Wannier functions of these superlattices have peculiar symmetry properties. We discuss the stability of the properties of such superlattices versus the electron in-plane motion. As a distinct fingerprint, the inter-sub-band magnetoabsorption spectrum for such superlattices is discussed.

DOI: 10.1103/PhysRevB.89.235301 PACS number(s): 73.21.Ac, 78.67.Pt

I. INTRODUCTION

Massless Dirac bands, electronic dispersion relations that are linear upon the wave vector in the vicinity of a high symmetry point in the Brillouin zone, are heavily researched because they lead to unusual physical properties [1,2]. The prototype of material that displays such linear dispersion relations is graphene. Here we will show that the very same linear dispersions occur for the unbound states of one-dimensional (1D) semiconductor superlattices [3] (SL), such as GaAs/Ga(Al)As, provided the layer thicknesses are appropriately chosen. In the following we will refer to such specific superlattices as Dirac SL's. The existence of gapless states (sub-band crossing) in the continuum of superlattices was briefly mentioned in Ref. [4] and their experimental evidence was first obtained by Sirtori et al. [5] by means of inter-sub-band absorption in (GA,In)As/(Al,In)As superlattices. Going beyond these studies we address the following issues here: (i) The occurrence of a linear dispersion with an associated Dirac point is discussed. (ii) The change in the parity property of the SL eigenstates and of their associated Wannier functions when crossing the Dirac point by a small change in the thicknesses is established. (iii) The stability of the Dirac point with respect to the electron in-plane motion, which is nontrivial as the longitudinal and in-plane motions are coupled in general, is discussed. Furthermore we present our results for the inter-sub-band magnetoabsorption where the Dirac SL's should be best evidenced.

II. ANALYTICAL RELATION FOR A DIRAC POINT

Within the present work we consider a binary SL made of a periodic stacking of layers A (well-acting material) and B (barrier-acting material) with thicknesses L_A , L_B . We denote $d = L_A + L_B$ as the SL period. We use parabolic dispersion relations in both kinds of layers characterized by effective masses m_A , m_B in the well and barrier, respectively [6] (including band nonparabolicity is doable if requested but

cumbersome and does not bring any new feature to the linear dispersion problem¹). We choose the energy origin at the bottom of the conduction band of the well-acting material and call V_b the barrier height. We note q the SL wave vector and concentrate on the electron motion along the growth axis for states that are propagating in both kinds of layers ($\epsilon \ge V_b$). The superlattice dispersion relation for a zero in-plane wave vector, i.e., at the sub-band edge, is therefore [6]:

$$\cos(qd) = \cos(k_A L_A) \cos(k_B L_B)$$
$$-\frac{1}{2} \left(\xi + \frac{1}{\xi}\right) \sin(k_A L_A) \sin(k_B L_B), \quad (1)$$

where

$$\xi = \frac{k_A m_B}{m_A k_B}, \quad k_A = \sqrt{\frac{2m_A \epsilon}{\hbar^2}}, \quad k_B = \sqrt{\frac{2m_B (\epsilon - V_b)}{\hbar^2}}.$$

In Eq. (1) one sees immediately that the energies $\epsilon_{jj'}$ which fulfill

$$k_A L_A = j\pi, \quad k_B L_B = j'\pi \tag{2}$$

with j and j' integers are solutions of the equation. If j+j' is even (odd) these energies are associated with qd=0 ($qd=\pi$). This double Fabry-Perot condition was mentioned to be associated with zero band gap in the SL dispersion relations [4,5,7]. This implies a definite relationship between L_A , L_B and V_b :

$$\frac{m_B j^2 \pi^2}{m_A L_A^2} - \frac{2m_B V_b}{\hbar^2} = \frac{j'^2 \pi^2}{L_B^2}.$$
 (3)

Hence, for masses that are not too different, L_B has to be larger than L_A if j = j'. We show in Fig. 1 the L_B

^{*}francesca.carosella@lpa.ens.fr

¹In the case of InAs/GaSb superlattices where the nonparabolicity is a mandatory ingredient to understand the hybridization between the InAs electrons states and the GaSb light hole states, all the results discussed in terms of Fabry-Perot conditions as well as of linear dispersions apply. The only ingredient that changes in Eq. (1) is the definition of the effective masses m_A and m_B , which must account for nonparabolicity effects [6].

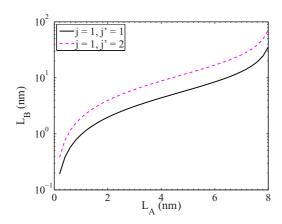


FIG. 1. (Color online) Barrier (L_B) versus well (L_A) thickness for the j=j'=1 resonance condition (dashed line) and for the j=1, j'=2 resonance condition (continuous line).

versus L_A curve for j=j'=1, and j=1 and j'=2 using the material parameters $m_A=0.07m_0$, $m_B=0.076m_0$, $V_b=80$ meV. These parameters correspond roughly to GaAs/Ga_{0.89} Al_{0.11}As SL's. A low barrier height will ensure that the Dirac bands can be easily optically probed and will affect significantly the carrier dynamics in the SL. In this work we will show the results of the calculations for two Dirac SL's structures with the parameters indicated above and either with $L_A=7$ nm and $L_B=12.92$ nm (satisfying the resonance condition j=j'=1), or with $L_A=6.6$ nm and $L_B=21.37$ nm (satisfying the resonance condition j=1, j'=2).

The very fact that both sines in Eq. (1) vanish when the resonance conditions [Eq. (2)] are satisfied implies that close to an energy $\epsilon_{jj'}$ the dispersion relations will be linear either in the vicinity of q=0 or $q=\pi/d$ and degenerate in one of these points. In fact letting $\epsilon=\epsilon_{jj'}+\eta$, with η very small, for j+j' odd and $q=\pi/d-Q$, with Qd small and positive, there is

$$\eta^{2} = \frac{Q^{2}d^{2}}{G_{jj'}},$$

$$G_{jj'} = \frac{m_{B}^{2}L_{B}^{4}}{\hbar^{4}j'^{2}\pi^{2}} + \frac{m_{A}^{2}L_{A}^{4}}{\hbar^{4}j^{2}\pi^{2}} + \left(\frac{jm_{B}L_{B}}{j'm_{A}L_{A}} + \frac{j'm_{A}L_{A}}{jm_{B}L_{B}}\right) \frac{m_{A}m_{B}L_{A}^{2}L_{B}^{2}}{\hbar^{4}jj'\pi^{2}} \tag{4}$$

On the other hand for j + j' even, in the vicinity of q = 0, we find a similar formula:

$$\eta^2 = \frac{q^2 d^2}{G_{ii'}},\tag{5}$$

where $G_{jj'}$ is the same as in Eq. (4). Hence, in contrast to a widespread belief, the dispersion relations of binary SL's can be linear in q in the vicinity of either the Brillouin zone center or the zone boundary provided the double Fabry-Perot conditions are fulfilled. The effective velocity corresponding to this linear dispersion close to $qd = \pi$ is $4.6 \times 10^5 m/s$ for the Dirac SL with j = 1, j' = 2 resonance. This average velocity for a $|p,q\rangle$ SL state is equal to $\langle p,q|\frac{p_z}{m_0}|p,q\rangle$ and coincides

numerically with $\frac{1}{\hbar} \frac{\partial \epsilon_p}{\partial q}$ in spite of the inapplicability of the usual one-band approximation to this degenerate case.

Note that for an arbitrary superlattice it is known [8] that the dispersion relations are the solution of the following equation:

$$\cos(qd) = f(\epsilon),\tag{6}$$

where $f(\epsilon)$ is a function of the energy. Hence, to get Dirac bands in an arbitrary superlattice, the function $f(\epsilon)$ must be such that in the vicinity of $\epsilon_c = \epsilon(q=0)$ or $\epsilon_b = \epsilon(q=\pi/d)$ there is

$$f(\epsilon) \approx 1 - \frac{(\epsilon - \epsilon_c)^2}{\delta_c^2}$$
 or $f(\epsilon) \approx -1 + \frac{(\epsilon - \epsilon_b)^2}{\delta_b^2}$, (7)

where δ_c and δ_b are constants. It is difficult to be more specific on general grounds since $f(\epsilon)$ is fixed by the potential profile in the superlattice unit cell. However, we note that the function $f(\epsilon)$ is usually larger or much larger than one when the electron wave is evanescent, thereby preventing Eq. (7) to be realized. In addition, we wish to point out that the existence of Dirac bands in a given superlattice family [which differs by the strength of the potential or by the period length as found, e.g., in the cosine-shaped potential $V(z) = V_b \cos(\frac{2\pi z}{d})$] is by no means guaranteed. Let us indeed consider the Dirac comb:

$$V(z) = V_0 L \sum_{n} \delta(z - nd), \tag{8}$$

where L is a length and d the period. It is easily found that

$$\cos(qd) = f(\epsilon) = \cos(kd) + \frac{m^* V_b L}{\hbar^2} \frac{\sin(kd)}{kd},$$

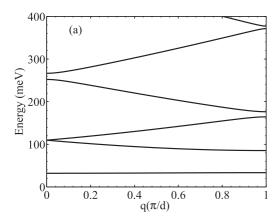
$$k = \sqrt{\frac{2m^* \epsilon}{\hbar^2}}.$$
(9)

It is still true that $kd = m\pi$, with m an integer, ensures $f(\epsilon_m) = (-1)^m$. However, at these energies it is impossible to simultaneously ensure $\frac{df}{d\epsilon}(\epsilon_m) = 0$. Hence, in general, a one-dimensional potential does not always admit Dirac bands. For that reason in the present article we study only the specific case of flat band binary superlattices.

We show in Fig. 2 the flat band binary SL dispersion relations $\epsilon_p(q)$ calculated for a j=j'=1 resonance and for a j=1, j'=2 resonance (the parameters for each structure are indicated above). As expected from the analytical calculation [Eq. (4) and Eq. (5)] we find sub-bands with linear dispersions and degenerate at q=0 or $q=\pi/d$. Specifically, for the SL with j=j'=1 resonance the second and third sub-bands are degenerate at q=0 and show linear dispersions close to the zone center. Conversely, for the SL with j=1, j'=2 resonance the third and fourth sub-bands are degenerate at $q=\pi/d$ and are Dirac-like close to the zone boundary. In both cases there is a single sub-band bound in the well that exhibits very little dispersion (less than 1 meV). The other sub-bands are regular SL sub-bands.

III. WANNIER FUNCTIONS AT THE DIRAC POINT

Moreover, the realization of a resonance condition in a SL influences dramatically the symmetry properties of the SL eigenstates and of their associated Wannier functions. Wannier functions can be constructed from the Bloch states, for SL's



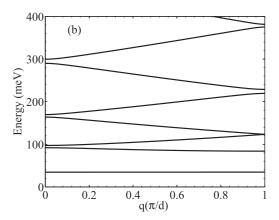


FIG. 2. Dispersion relations for a GaAs/Ga(Al)As SL verifying the resonance condition (a) j = j' = 1 ($V_b = 80$ meV, $L_A = 7$ nm, $L_B = 12.92$ nm) and (b) j = 1, j' = 2 ($V_b = 80$ meV, $L_A = 6.6$ nm, $L_B = 21.37$ nm). Notice that in both cases the first sub-band is bound and is almost dispersionless. In (a) the second and third sub-bands are Dirac-like, while in (b) the third and fourth sub-bands are Dirac-like.

see, e.g., Refs. [9,10], where the optimization of their spatial localization was addressed. We show in Fig. 3 a comparison between the Wannier functions of a Dirac SL (j = j' = 1)and those of SL's with nearby layer thicknesses, the SL period being kept the same. On general grounds [9,10], the Wannier functions for a superlattice with inversion symmetry should be symmetric or antisymmetric with respect to one of the symmetry points (center of well or center of barrier). While the Wannier function of the bound sub-band is about the same in the three SL's, being symmetrical with respect to the center of the well, the symmetry property of sub-bands with energy larger than V_b are interchanged in the sequence of SL's. In the case of the wider well ($L_A = 8$ nm), the Wannier function of the second sub-band is antisymmetric with respect to the center of the well, and the Wannier function of the third sub-band is symmetric with respect to the center of the barrier. Reducing the well width (and increasing the barrier width) increases

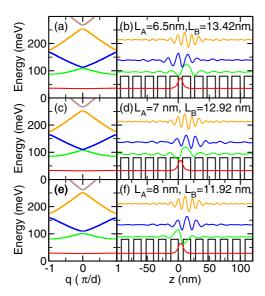


FIG. 3. (Color online) Wannier functions calculated according to the procedure of Ref. [10] for a sequence of superlattices, where the middle one with $L_A=7$ nm, $L_B=12.92$ nm satisfies the Dirac condition.

the energy of the well-like state and decreases the energy of the barrierlike state, so that the sequence is opposite at $L_A = 6.5$ nm. In between (for the Dirac SL at $L_A = 7$ nm) the symmetries of these Wannier functions are becoming ill defined. Furthermore, the Wannier functions for the Dirac SL (evaluated by the procedure of Ref. [10]) are badly localized and we cannot observe an exponential decay numerically. This is a direct consequence of the fact that the localization of Wannier states is related to the width of the band gap [9]. Thus general calculation schemes, such as the one given in Ref. [10], are only valid for isolated bands.

IV. ABSORPTION SPECTRUM

Linear dispersions imply a number of distinctive features. For instance, the inter-sub-band absorption line shape will be drastically modified compared to the usual divergences at sub-band extrema q=0 or $q=\pi/d$ expected for a 1D free particle with quadratic dispersion relation [11]. In the following, we discuss the inter-sub-band absorption starting from the ground sub-band of the superlattice. We assume a strong magnetic field has been applied parallel to the growth axis in order to Landau quantize the in-plane motion ($\omega_c \approx 16.4$ meV at B=10 T for GaAs). Under such circumstances, the electronic motion is free only along the growth axis. The optical selection rules are that the electric vector of the wave has to be parallel to the growth axis and that the Landau quantum numbers are conserved for the in-plane motion and that the transitions are vertical in the reciprocal space.

We show in Fig. 4 the q dependence of the modulus of the inter-sub-band p_z matrix element (from ground sub-band to higher-energy sub-bands) for the 6.6 nm/21.37 nm SL satisfying the j=1, j'=2 resonance condition [see Fig. 2(b) for the dispersion relation]. In this superlattice there exists an almost dispersionless bound sub-band E_1 at about 34 meV. The first continuum sub-band E_2 is regular; hence the dispersions are parabolic in the vicinity of both q=0 and $q=\pi/d$ and there is no degeneracy. Thus, at q=0 ($q=\pi/d$) the superlattice wave functions should have the same (opposite) parities with respect to the centers of the layers [12]. As a result the p_z inter-sub-band matrix elements vanish at q=0. This reasoning also applies to the other regular sub-bands. For

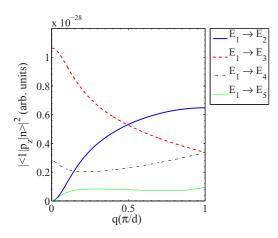


FIG. 4. (Color online) Squared dipole matrix element (p_z) between the ground bound sub-band E_1 and the continuum sub-bands E_2 , E_3 , E_4 , E_5 . The Dirac sub-bands are E_3 and E_4 . The calculations are done for the SL satisfying j = 1, j' = 2 resonance condition.

the Dirac sub-bands with linear dispersions near $q = \pi/d$, we have found no such cancellations. Instead we find the same matrix elements at $q = \pi/d$ as if sub-band 4 were the continuation of sub-band 3.

The inter-sub-band absorption line shape for the 6.6 nm/ 21.37 nm SL is shown in Fig. 5. This absorption spectrum is numerically calculated by replacing the delta function expressing the energy conservation by a Lorentzian function with a broadening parameter of 0.2 meV. This choice of broadening parameter is kept through all the paper. In Fig. 5 the first peak corresponds to $E_1 \rightarrow E_2$ optical transitions around $q = \pi/d$. The transition $E_1 \to E_2$ at q = 0 is parity forbidden and thus the associated absorption line is absent. The second peak corresponds to the $E_1 \rightarrow E_3$ transition at q=0. It extends up to 129.1 meV, which is the $E_1 \rightarrow E_4$ transition at q = 0. There is no hint of any feature around 89.2 meV, which would correspond to the transitions $E_1 \rightarrow E_3$ and $E_1 \to E_4$ at $q = \pi/d$. Indeed, it can be readily checked that in the vicinity of this energy the absorption line shape is a plateau (with the same amplitude before and after the critical energy). Finally, the $E_1 \rightarrow E_5$ transition starts smoothly at q = 0 (Fig. 4) because it is parity forbidden at the zone center

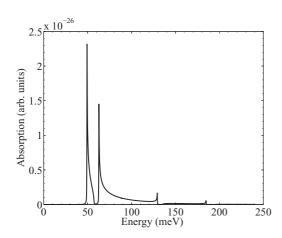


FIG. 5. Absorption spectrum from ground sub-band towards higher energy sub-bands for the 6.6 nm / 21.37 nm SL (j = 1, j' = 2).

and ends up with a small singularity in the absorption spectrum at 184.7 meV, because the dipole matrix elements of $E_1 \rightarrow E_5$ is very small for any q. A similar analysis could be made for the absorption spectrum of the superlattice satisfying the j=j'=1 resonance condition.

It is interesting to compare what happens to the optical spectra when the layer thicknesses are changed slightly around those that realize a Dirac SL. Figure 6 shows the inter-sub-band absorption for the Dirac SL with well thickness $L_A=7\,\mathrm{nm}$ and for two other SL's having the same period length 19.92 nm but well thickness of respectively 6.5 nm and 8 nm (where

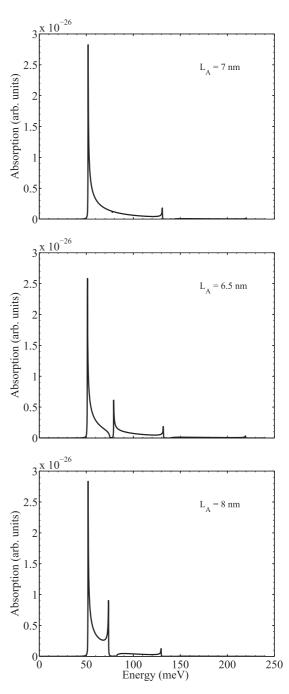
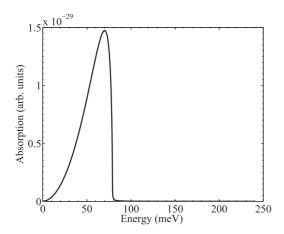


FIG. 6. Comparison between the absorption coefficient of three SL's with the same period d=19.92 nm. The Dirac SL corresponds to j=j'=1 and $L_A=7$ nm.



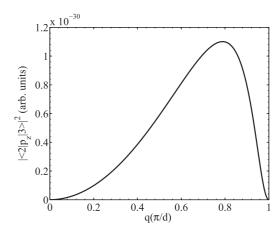


FIG. 7. Absorption spectrum (left) and p_z matrix element (right) for the optical transition from the lowest energy Dirac band to the higher energy one of the 7 nm /12.92 nm SL.

no resonance condition is satisfied). As shown in Fig. 2(a) the Dirac SL satisfying the j = j' = 1 resonance condition has sub-bands E_2 and E_3 degenerate at q=0 and located 77.8 meV above the ground sub-band. The three SL's share common optical features that are associated with the $E_1 \rightarrow$ E_2 and $E_1 \rightarrow E_3$ optical absorption at $q = \pi/d$ (peaks at about 51 meV and 131 meV). Near 77 meV the SL's with $L_A = 6.5$ nm and 8 nm show a transparency window. The 6.5 nm SL has a parity forbidden transition $E_1 \rightarrow E_2$ at q = 0at the beginning of the transparency region while this q = 0transition is allowed for the next absorption band (peak at 80 meV). The reverse situation takes place for the SL with $L_A = 8$ nm, the q = 0 optical transition being allowed (peak at 72.8 meV) then forbidden on each sides of the transparency region. The Dirac SL with $L_A = 7$ nm resolves this parity change by showing no particular optical features (in particular no transparency region) at about 77 meV where the $E_1 \rightarrow E_2$ absorption ends and the $E_1 \rightarrow E_3$ absorption starts.

Optical transitions between the Dirac sub-bands are allowed but weak as shown in the left panel of Fig. 7 for the j=j'=1 SL. The corresponding p_z matrix element is shown in the right panel of Fig. 7 and vanishes both at q=0, because the degeneracy point is shown at the zone center, and at $q=\pi/d$ for parity reasons.

V. DISCUSSION

A. Stability against varying in-plane wave vector

An interesting question is to examine whether the sub-band edge persists at nonzero in-plane wave vector [7]. Although the effective mass mismatch is small in the material we have chosen, the existence of degenerate bands either at q=0 or $q=\pi/d$ may invalidate the usual perturbative treatments. When there is a position-dependent effective mass (piecewise constant), we need to find the eigenstates of the following Hamiltonian in presence of a magnetic field:

$$H = p_z \left(\frac{1}{2m(z)}\right) p_z + V_b(z) + \frac{1}{2m(z)} \left[p_x^2 + (p_y + eBx)^2 \right].$$

Sensu stricto, H is not separable in z and (x,y). However, one feels that if the effective masses are not too different this nonseparability is not so important. Let us indeed split H into a separable H_0 and a term supposed to be small. We let

$$\frac{1}{m(z)} = \left\langle \frac{1}{m} \right\rangle + \left(\frac{1}{m(z)} - \left\langle \frac{1}{m} \right\rangle \right),\tag{11}$$

where $\langle \frac{1}{m} \rangle$ is not yet defined. The difference inside parentheses is expected to be small. Under such a circumstance we get:

$$H = H_0 + \delta H$$

$$H_0 = p_z \left(\frac{1}{2m(z)}\right) p_z + V_b(z) + \frac{1}{2} \left(\frac{1}{m}\right) \left[p_x^2 + (p_y + eBx)^2\right],$$

$$\delta H = \frac{1}{2} \left(\frac{1}{m(z)} - \left\langle \frac{1}{m} \right\rangle \right) \left[p_x^2 + (p_y + eBx)^2 \right]. \tag{12}$$

The eigenstates and eigenvalues of H_0 are known:

$$\langle \overrightarrow{r} | n, k_y, p, q \rangle = \frac{1}{\sqrt{L_y}} \exp(ik_y y) \phi_n(x + \lambda^2 k_y) \chi_{p,q}(z),$$

$$\epsilon_{n,k_y,p,q}^0 = \epsilon_p(q) + (n + 1/2) \hbar \langle \omega \rangle, \tag{13}$$

where $\langle \omega \rangle = eB\langle \frac{1}{m} \rangle$ and $\lambda = \sqrt{\frac{\hbar}{eB}}$. Now, in order to make the effects associated with δH to be as small as possible, we impose that the first-order correction to $\epsilon^0_{n,k_y,p,q}$ vanishes:

$$\langle n, k_{y}, p, q | \delta H | | n, k_{y}, p, q \rangle$$

$$= \left(n + \frac{1}{2} \right) \hbar e B \langle p, q | \left(\frac{1}{m(z)} - \left(\frac{1}{m} \right) \right) | p, q \rangle$$

$$= \left(n + \frac{1}{2} \right) \hbar \langle \omega \rangle \left(\langle p, q | \frac{1}{m(z) \langle \frac{1}{m} \rangle} | p, q \rangle - 1 \right) = 0. \quad (14)$$

Hence, the unknown $\langle \frac{1}{m} \rangle$ should be chosen such that $\langle \frac{1}{m} \rangle = \langle p,q | \frac{1}{m} | p,q \rangle$ if one wants the lack of separation between z and (x,y) motion to be minimized. In practice, it is enough to ensure the equality in one elementary cell since the perturbation will collect all the cells' responses but also since the eigenstates are Bloch states. Implicit in the previous reasoning is the nondegeneracy of the state $|p,q\rangle$. This is the case for most of the SL eigenstates except for the Dirac states.

In the latter case we shall *a priori* define a $\langle \frac{1}{m} \rangle = \frac{L_A}{m_A} + \frac{L_B}{m_B}$ and study the effect of δH between two degenerate Dirac states. For the sake of definiteness, we shall study the effect of δH at $q=\pi/d$ for a $j=1,\ j'=2$ resonance of the unperturbed Hamiltonian. Due to the twofold degeneracy, there is some room to define the two eigenfunctions where to project δH . These are

$$\chi_{\pi/d}^{(1)} = M \begin{cases} -\sin\frac{\pi u}{L_A} & -\frac{L_A}{2} \leqslant u \leqslant \frac{L_A}{2} \\ +\cos\frac{2\pi v}{L_B} & -\frac{L_B}{2} \leqslant v \leqslant \frac{L_B}{2} \end{cases}$$

$$\chi_{\pi/d}^{(2)} = M \begin{cases} -\cos\frac{\pi u}{L_A} & -\frac{L_A}{2} \leqslant u \leqslant \frac{L_A}{2} \\ +\xi \sin\frac{2\pi v}{L_B} & -\frac{L_B}{2} \leqslant v \leqslant \frac{L_B}{2} \end{cases}$$
(15)

where u and v refer to the position of the electron in layer A and B respectively and measured from the centers of the layers. M and N are constants obtained by normalizing the states in a SL period. With these wave functions one finds readily that δH has the following matrix elements:

$$\begin{split} &\langle \chi^{(1)} | \, \delta H \, | \chi^{(1)} \rangle \\ &= \langle \chi^{(1)} | \, \delta H \, | \chi^{(2)} \rangle = 0, \quad \langle \chi^{(2)} | \, \delta H \, | \chi^{(2)} \rangle \\ &= \left(n + \frac{1}{2} \right) \frac{\hbar \langle \omega \rangle}{\left\langle \frac{1}{m} \right\rangle} \frac{L_A L_B}{L_A + L_B} \left(\frac{1}{m_A} - \frac{1}{m_B} \right) \frac{1 - \xi^2}{L_A + \xi^2 L_B} \end{split}$$

$$(16)$$

with $m_A=0.07m_0$, $m_B=0.077m_0$, where m_0 is the free electron mass, $L_A=6.6$ nm, $L_B=21.3$ nm there is $\xi=1.752$ and $\langle \chi^{(2)} | \delta H | \chi^{(2)} \rangle = A(n+\frac{1}{2})\hbar \langle \omega \rangle$ with $A=1.41\times 10^{-2}$. At B=10T and for n=2 there is: $(n+\frac{1}{2})\hbar \langle \omega \rangle = 38.3$ meV. Hence the shift is -0.5 meV. This value is indeed very small (actually much smaller than a typical broadening). Thus, for the material parameters considered here the stability of Dirac feature against the in-plane wave vector is ensured. Note that the conclusion may have to be reconsidered if the effective mass mismatch is more severe like in Ga(In)As/Al(In)As

B. Impact on Bloch oscillations

The shape of the Dirac bands suggests in a semiclassical scenario of the Bloch oscillations ($\hbar dq/dt = -eF$, with F the electric field) that Dirac bands should be associated with an angular Bloch frequency of $eFd/2\hbar$. This is half the common

value, as the carrier need to transverse two times the Brillioun zone, before the origin is reached again. However, it is not at all obvious that a semiclassical analysis applies to a situation where there is no gap between the two bands [13,14]. In order to observe Bloch oscillations, a sufficiently large electric field is needed, so that the Bloch frequency surpasses the scattering rate. This would lead to large Zener tunneling [15] for the small gaps in the superlattices considered and thus makes the observation difficult in actual semiconductor superlattices. Optical lattices [16] with their absence of scattering may render the observation of Wannier quantization in Dirac SL's much easier.

C. Dirac bands and inversion symmetry

It is worth pointing out that the existence of Dirac bands in a binary SL is not related to the fact that the SL potential energy is centrosymmetric with respect to the center of one or the other layer that build the SL unit cell. Actually, we have found Dirac bands in the case of a polytype (ternary ABC superlattice) where the SL potential is noncentrosymmetric. In quaternary superlattices, one may even find a Dirac band between the first two bands, as indicated by numerical findings in Fig. 5 of Ref. [17].

VI. CONCLUSION

Previous works proved the existence of one-dimensional gapless Dirac bands in semiconductor superlattices provided multiple Fabry-Perot conditions are fulfilled. In the present work we show that the dispersion relations close to the crossing point are linear. These Dirac SL's lay at the boundary of the SL parameters where the symmetry of the Wannier function changes. The existence of gapless Dirac bands implies interesting optical features that partly result from density of states considerations but more importantly reflect the change in the symmetry properties of the SL states. We also discussed the stability of the properties of Dirac SL's against varying in-plane wave vector.

ACKNOWLEDGMENTS

We thank J. Dalibard and C. Sirtori for useful discussions. The work at Lund University has been supported by the Swedish Research Council.

^[1] A. H. Castro Neto, F. Guinea, N. M. R. Peres, K. S. Novoselov, and A. K. Geim, Rev. Mod. Phys. 81, 109 (2009).

^[2] M. Orlita and M. Potemski, Semicond. Sci. Technol. 25, 063001 (2010).

^[3] L. Esaki and R. Tsu, IBM J. Res. Dev. 14, 61 (1970).

^[4] G. Bastard, Wave Mechanics Applied to Semiconductor Heterostructures, Monographies de physique (Les Éditions de Physique, Les Ulis, 1988).

^[5] C. Sirtori, F. Capasso, D. L. Sivco, and A. Y. Cho, Appl. Phys. Lett. 64, 2982 (1994).

^[6] G. Bastard, Phys. Rev. B 24, 5693 (1981); 25, 7584 (1982).

^[7] G. Bastard, J. Brum, and R. Ferreira, in *Semiconductor Heterostructures and Nanostructures*, Solid State Physics, Vol. 44, edited by H. Ehrenreich and D. Turnbull (Academic Press, New York, 1991), pp. 229–415.

^[8] N. W. Ashcroft and N. D. Mermin, *Solid State Physics* (Holt, Rinehart and Winston, New York, 1976).

^[9] W. Kohn, Phys. Rev. 115, 809 (1959).

^[10] A. Bruno-Alfonso and D. R. Nacbar, Phys. Rev. B 75, 115428 (2007).

^[11] M. Helm, W. Hilber, T. Fromherz, F. M. Peeters, K. Alavi, and R. N. Pathak, Phys. Rev. B 48, 1601 (1993).

^[12] P. Voisin, G. Bastard, and M. Voos, Phys. Rev. B 29, 935 (1984).

- [13] G. Bastard, R. Ferreira, S. Chelles, and P. Voisin, Phys. Rev. B **50**, 4445 (1994).
- [14] A. M. Bouchard and M. Luban, Phys. Rev. B 52, 5105 (1995).
- [15] S. Glutsch, Phys. Rev. B 69, 235317 (2004).

- [16] E. Haller, R. Hart, M. J. Mark, J. G. Danzl, L. Reichsöllner, and H.-C. Nägerl, Phys. Rev. Lett. 104, 200403 (2010).
- [17] J. Y. Romanova, E. V. Demidov, L. G. Mourokh, and Y. A. Romanov, J. Phys.: Condens. Matter **23**, 305801 (2011).